U.S. DEPARTMENT OF ENERGY | Office of Science

DOE/SC-CM-16-004

FY 2016 Fourth Quarter Performance Metric: Use a coupled climate model, including a dynamic ice-sheet model, to estimate the impacts of climate change on the decadal-to-century-scale evolution of the Antarctic ice sheet

October 2016

DISCLAIMER

This report was prepared as an account of work sponsored by the U.S. Government. Neither the United States nor any agency thereof, nor any of their employees, makes any warranty, express or implied, or assumes any legal liability or responsibility for the accuracy, completeness, or usefulness of any information, apparatus, product, or process disclosed, or represents that its use would not infringe privately owned rights. Reference herein to any specific commercial product, process, or service by trade name, trademark, manufacturer, or otherwise, does not necessarily constitute or imply its endorsement, recommendation, or favoring by the U.S. Government or any agency thereof. The views and opinions of authors expressed herein do not necessarily state or reflect those of the U.S. Government or any agency thereof.

Contents

1.0 Product Definition 1
2.0 Product Documentation 1
3.0 Results 2
4.0 References 8

Figures

1. Schematic from Spence et al. showing changes in ocean density structure near coastal Antarctica following changes in wind stress and coastal Ekman pumping 3
2. Difference in zonal ocean speed (control minus perturbed winds simulation) 4
3. Antarctic sub-ice-shelf mass balance anomalies calculated from the difference between submarine melt rates in the control simulation and the simulation with perturbed winds. Increased submarine melting, due to an increase in warm-water upwelling in the perturbed winds simulation, manifests as a more negative ice-shelf basal mass balance 4
4. Modeled surface speed on variable-resolution Antarctica ice sheet mesh 5
5. Difference in modeled ice surface speed over West Antarctica after 100 years of forcing with melt rates from the perturbed Southern Ocean winds simulation, relative to the control simulation 6
6. Difference in modeled ice surface speed over Wilkes Land and Queen Mary Land after 100 years of forcing with melt rates from the perturbed Southern Ocean winds simulation, relative to the control simulation 7
7. Difference in total ice volume loss when Antarctic ice sheet model is forced using submarine melt rates diagnosed from the simulation with perturbed Southern Ocean winds versus the control simulation 7

1.0 Product Definition

Future sea-level rise from the Antarctic ice sheet is expected to be a strong function of the integrity of Antarctica's fringing ice shelves, which limit the flux of ice from the continent to the surrounding oceans (Fürst et al., 2016). This hypothesis is supported by both observations (e.g., Scambos et al., 2014) and modeling (e.g., Gudmundsson, 2013; DeConto and Pollard, 2016). One of the primary processes by which Antarctica's ice shelves are vulnerable to degradation is increases in submarine melting, which occur when warm, intermediate-depth ocean water is brought into contact with ice shelves through changes in circulation and upwelling (e.g., Hellmer et al., 2012). At present, a key oceanographic feature limiting such upwelling onto the Antarctic continental shelf is the "Antarctic Slope Front", a narrow region of steeply tilted, constant-density surfaces near coastal Antarctica. This density structure is affected by the large-scale structure of the Southern Ocean westerly wind field. Anticipated changes in this wind field as a result of anthropogenic climate change (Fyfe et al., 2007; Zheng et al., 2013) are projected to weaken the Antarctic Slope Front, with concomitant increases in Antarctic coastal warm water upwelling (Spence et al., 2014). Using a coupled climate model and a dynamic ice sheet model, we estimate the impact of these changes on the submarine melting of Antarctic ice shelves and, in turn, on the dynamics of grounded ice currently buttressed by these same ice shelves; over 100 years, we estimate ~30 mm of sea-level rise as a result of these processes.

2.0 Product Documentation

The ACME climate model allows for coupled, global simulations that include ocean circulation within sub-ice-shelf cavities, allowing for the calculation of sub-ice-shelf melting and freezing rates. Changes in these melting rates occur as a function of changes in ocean circulation, which impact melting rates through the delivery of warm, salty, intermediate-depth waters to ice-shelf cavities (Jacobs et al., 2011). A critical oceanographic feature that limits such changes is the Antarctic Slope Front – a region of steeply inclined isopycnals near the Antarctic coast – which prevents warm intermediate waters from accessing the continental shelves. Degradation of the Antarctic Slope Front is anticipated under future climate change as a result of far field changes in the Southern Hemisphere Westerly winds, which drive the Antarctic Circumpolar Current, flowing West to East. Under future climate warming scenarios, the Westerlies are projected to increase in strength and shift farther south, resulting in a *decrease* in the strength of Antarctica coastal Easterly winds that drive the Antarctic Coastal Countercurrent (flowing West to East). In turn, this change reduces Ekman transport towards the coast and the downwelling of cold, fresh water, which helps maintain the Antarctic Slope Front (Spence et al., 2014).

We use the ACME climate model, climate perturbation experiments, and a dynamic ice-sheet model to simulate the impacts of these future changes on mass loss and sea-level rise from the Antarctic ice sheet. Following a similar set of experiments to those conducted by Spence et al. (2014), we conduct two simulations: (1) a control simulation with atmospheric forcing taken from the standard "normal year" (Yeager and Large, 2009), and (2) a perturbation simulation in which normal-year forcing includes winds perturbed to simulate the anticipated poleward shift and strengthening of the Westerlies. Unlike Spence et al. (2014), we include sub-ice-shelf cavities in our simulations, allowing us to calculate sub-ice-shelf melt rates, which we then use to force evolution of a dynamic ice-sheet model. We show that the applied wind perturbations result in changes in ocean circulation (a *reduction* in the speed of the coastal countercurrent)

and sub-ice-shelf melt rates (an *increase* in warm water upwelling and sub-ice-shelf melting) as anticipated by previous results of Spence et al. (2014). Differences between our control simulation and our perturbed-winds simulation indicate that ice-sheet volume loss is greater in the perturbation simulation. We estimate a potential mass loss from the Antarctic ice sheet equivalent to ~90 mm of sea-level over 100 yrs. Because some of this mass loss occurs within portions of the ice sheet already displacing global sea level, ~30 mm of this mass loss would contribute directly to global sea-level rise.

3.0 Results

Via a complex set of processes, the large-scale Southern Ocean wind field – defined primarily by strong Westerly winds that drive the Antarctic Circumpolar Current from West to East – helps to control the present-day location and strength of the of the "Antarctic Slope Front", an ocean density structure that limits vertical mixing of warm, intermediate depth waters (Circumpolar Deep Water, or "CDW", in the Ross and Bellingshausen Seas, and analogous bodies of water elsewhere around the continent) up onto the continental shelves where they can lead to large increases in the rate of sub-ice-shelf melting (e.g., Jacobs et al., 2011). This density structure is maintained by downward Ekman pumping of cold, fresh surface waters along the Antarctic coast as a result of the Antarctic Coastal Current (flowing from East to West), which in turn is driven by strong Easterly winds around the coast of Antarctica. These coastal Easterly winds are affected by the location and strength of the Westerly winds farther north, and thus changes in the Westerly winds can also affect the strength of the Antarctic Slope Front.

A trend towards a positive index of the Southern Annular Mode (SAM) has been observed since the 1950's and is associated with a strengthening and poleward shifting of the Southern Hemisphere circumpolar Westerlies (Thompson and Solomon, 2002; Fyfe et al., 2007). This positive trend, which is projected to continue into the future, is a robust feature of climate model simulations under anthropogenic forcing (Zheng et al., 2013). This projected change has significant implications for the strength of the Antarctic Slope Front; a positive trend in the SAM leads to a continued strengthening and poleward shifting of the circumpolar Westerlies, a reduction in the strength and extent of the coastal Easterlies and the Antarctic Coastal Current, and a consequent decrease in downward coastal Ekman pumping. As illustrated in Figure 1, this set of linked processes is likely to result in degradation of the Antarctic Slope Front, allowing warm intermediate water masses easier access to the continental shelf and potentially increasing sub-ice-shelf melt rates. Previous simulations using a high-resolution ocean model with perturbed wind forcing have been used to explore this set of coupled-climate processes. Spence et al. (2014) simulated anticipated Southern Ocean wind changes under future anthropogenic climate change by both increasing the strength of the circumpolar Westerlies and shifting them poleward. They demonstrated (1) a decrease in the speed of the Antarctic Coastal Current and downward Ekman pumping, (2) resulting in degradation of the Antarctic Polar Front, and (3) increased upwelling of warm, intermediate depth waters around coastal Antarctica.

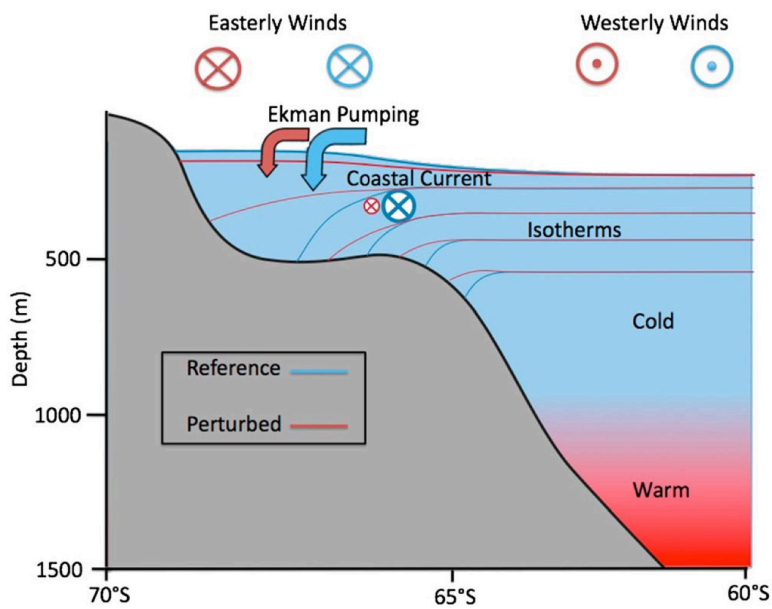

Figure 1. Schematic from Spence et al. (2014) showing changes in ocean density structure near coastal Antarctica following changes in wind stress and coastal Ekman pumping. The resulting degradation of the Antarctic Slope Front (region of tilted density surfaces near the coast) allows warm intermediate-depth waters easier access to the continental shelves.

With an aim to assess the potential for changes in ice-sheet volume over time, we conduct a similar set of experiments, but using the ACME coupled climate model, which includes additional critical processes relative to previous efforts. The model configuration uses variable-resolution ocean and sea-ice models (60 km at the Equator decreasing to 30 km at the poles) and allows for ocean circulation in sub-ice-shelf cavities (floating extensions of the Antarctic ice sheet). The ocean and ice sheet exchange heat and freshwater fluxes via a set of thermodynamic boundary-layer equations (Holland and Jenkins, 1999; Jenkins et al., 2010), and changes in submarine melt rates resulting from increased warm-water upwelling are used to force evolution of a dynamic ice-sheet model. Atmospheric forcing is provided by two CORE "normal year" (NY; Yeager and Large, 2009) data sets. In our control simulation, we use the standard CORE-NY data set (hereafter referred to as the "control simulation"), while in a second simulation, we use a perturbed CORE-NY data set in which Southern Hemisphere winds are altered as anticipated under anthropogenic climate change (as discussed above and in further detail in Spence et al. [2014]).

In Figure 2, we show zonal wind velocity differences around coastal Antarctica from our two simulations. In the CORE-NY simulation using perturbed winds (hereafter, "perturbed-winds simulation"), there is a clear reduction in the east-to-west zonal ocean speed relative to the control simulation (negative values contoured blue in Figure 2), which is in turn associated with a simulated reduction in downward Ekman pumping, and thus a reduction in the strength of the Antarctic Polar Front. The resultant change in sub-ice-shelf melt rates relative to the control simulation is shown in Figure 3 (displayed as ice-shelf mass balance, so that a negative mass balance corresponds to an increased sub-ice-shelf melt rate). While some regions show decreased melt rates (red = an increase in ice-shelf mass balance), on the whole, sub-ice-shelf melt rates have increased (blue = a decrease in ice-shelf mass balance) as a result of decreased downward Ekman pumping and increased upwelling of warm, intermediate-depth waters.

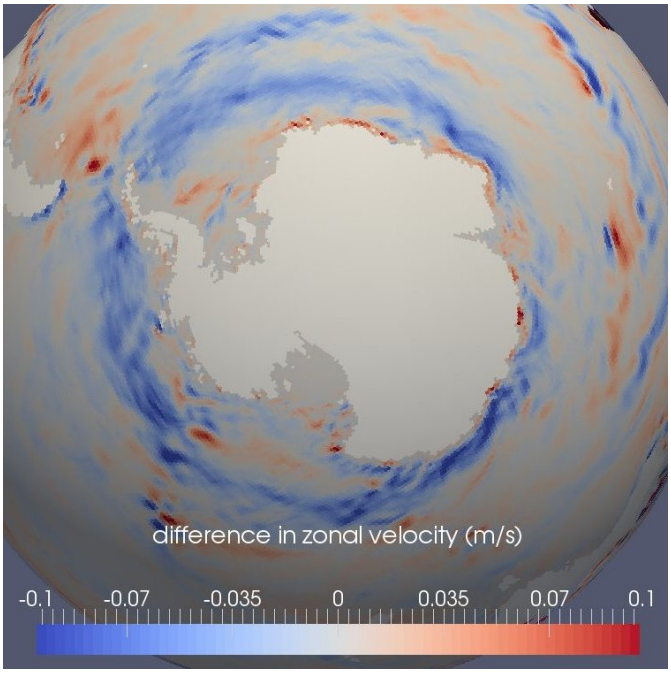

Figure 2. Difference in zonal ocean speed (control minus perturbed winds simulation). Negative values (blue) near the coast indicate a reduction in the speed of the east-to-west flowing Antarctic Coastal Current, which leads to decreases in coastal downwelling of cold, fresh water that helps to maintain the Antarctic Slope Front.

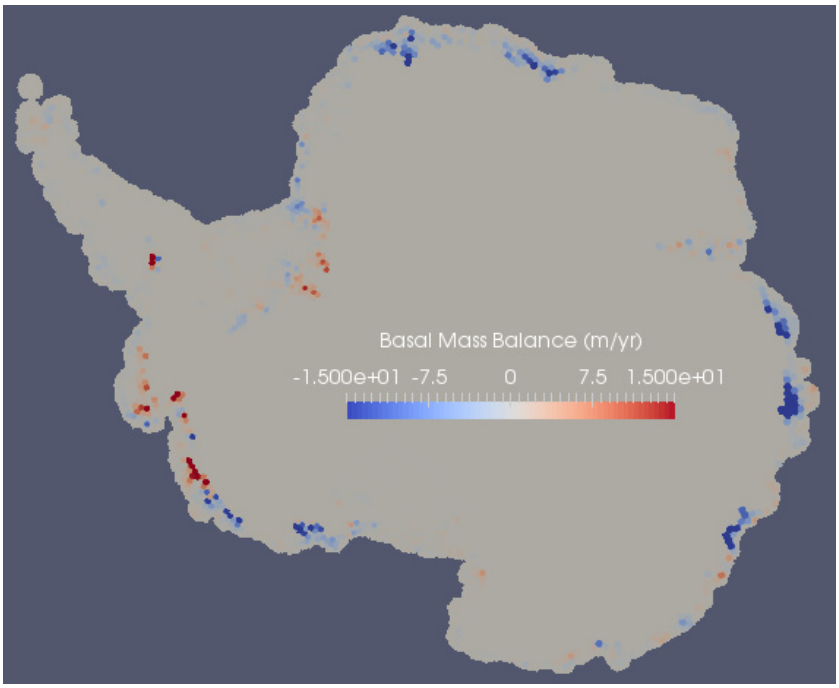

Figure 3. Antarctic sub-ice-shelf mass balance anomalies calculated from the difference between submarine melt rates in the control simulation and the simulation with perturbed winds. Increased submarine melting, due to an increase in warm-water upwelling in the perturbed winds simulation, manifests as a more negative (blue) ice-shelf basal mass balance.

The sub-ice-shelf melt rate patterns from these two simulations are used to force two different ice-sheet evolution simulations, each for 100 years; one simulation is forced by melt rates from the control simulation and a second simulation is forced by melt rates from the perturbed winds simulation. The ice-sheet model uses a variable-resolution mesh, ranging in resolution from 14 km deep in the ice-sheet interior, to ~4 km in regions of dynamic complexity, such as ice streams and grounding lines – the transition from grounded to floating ice (Figure 4).

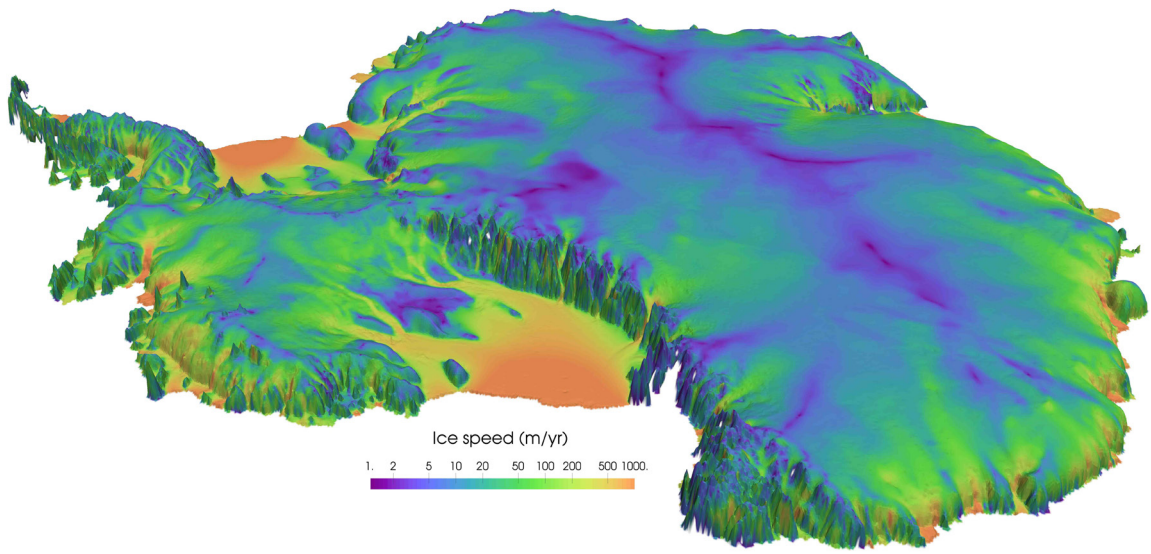

Figure 4. Modeled surface speed on variable-resolution Antarctica ice sheet mesh. PDE-constrained optimization methods are used to provide a best match between observed and modeled velocities.

In Figures 5, 6, and 7 we show the impact of the increased melt rates on the ice sheet in terms of changes in ice speed, ice thickness, and overall ice volume. In the simulation with perturbed winds, the increased submarine melt rates lead to increased ice-shelf thinning, a reduction in the ice shelves' ability to "buttress" the flow of ice upstream, and an increase in flow speeds on grounded ice upstream from ice shelves (top and left panels of Figure 5 and Figure 6, respectively). In turn, increased flow speeds lead to increased ice thinning (bottom and right panels of Figure 5 and Figure 6, respectively). Increased flow speeds and thinning are seen in both West and East Antarctica, and lead to an overall reduction in Antarctic ice volume over time. In Figure 7, we show the time series of the difference in ice volume for the two simulations. A positive change (provided in units of sea-level equivalent volume change) indicates that the rate of volume loss is larger at all times for the simulation with perturbed winds and increased submarine melt rates. This applies for both floating and grounded ice portions of the ice sheet. The overall difference in ice-sheet volume after 100 years of forward model simulation is on the order of ~90 mm of sea-level equivalent (Figure 7). However, only ~30 mm of this would contribute directly to sea-level rise, as ~2/3 of the volume difference between our two simulations occurs within regions of the ice sheet that are already displacing sea level (i.e., as floating ice shelves or as ice grounded below sea level).

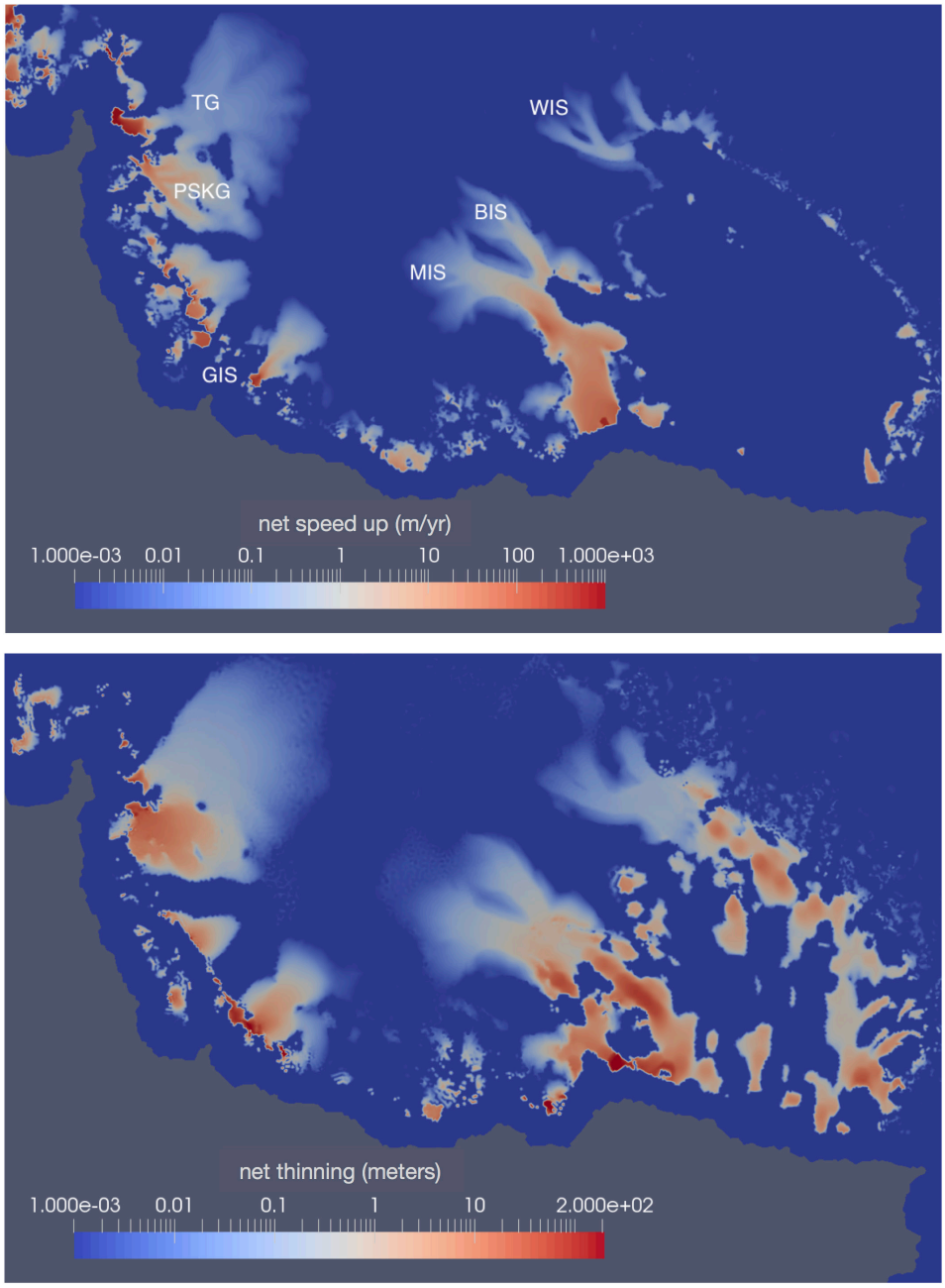

Figure 5. (top) Difference in modeled ice surface speed over West Antarctica after 100 years of forcing with melt rates from the perturbed Southern Ocean winds simulation, relative to the control simulation (speed differences, on a log10 scale, are positive where greater than in the control simulation). (bottom) As in top panel but for ice thickness. Labels for specific glacier catchments are: Thwaites Glacer (TG), Pope, Smith, and Kohler Glaciers (PSKG), Getz Ice Shelf (GIS), MacAyeal, Bindschadler, and Whillans Ice Streams (MIS, BIS, WIS).

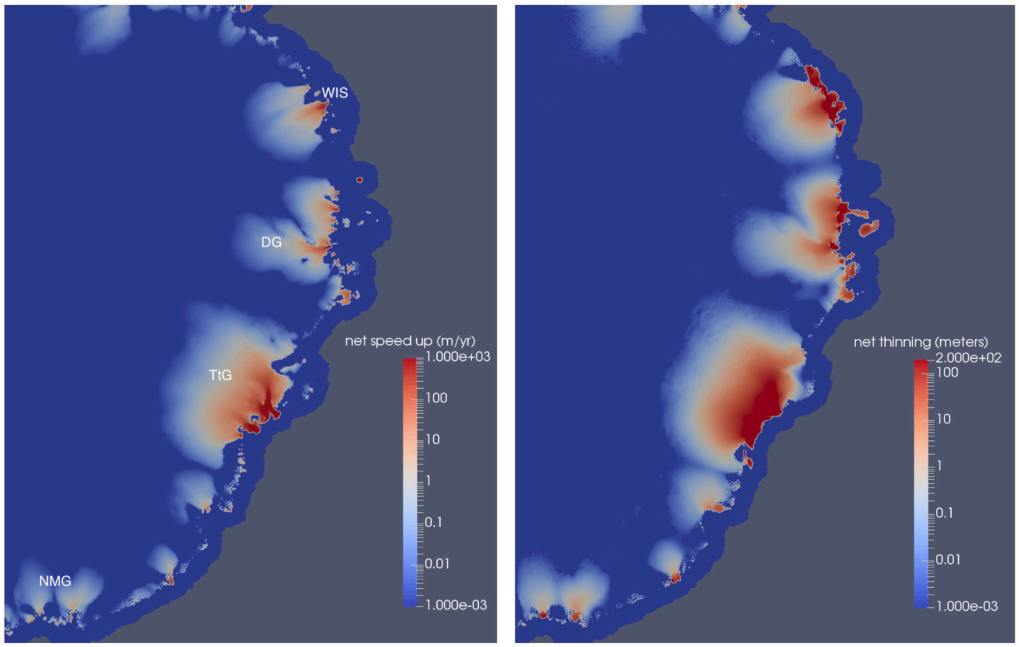

Figure 6. (left) Difference in modeled ice surface speed over Wilkes Land and Queen Mary Land (East Antarctica) after 100 years of forcing with melt rates from the perturbed Southern Ocean winds simulation, relative to the control simulation (speed differences, on a log10 scale, are positive where greater than in the control simulation). (right) As in left panel but for ice thickness. Labels for specific glacier catchments are: West Ice Shelf (WIS), Denemen Glacier (DG), Totten Glacier (TtG), and Ninis/Mertz Glaciers (NMG).

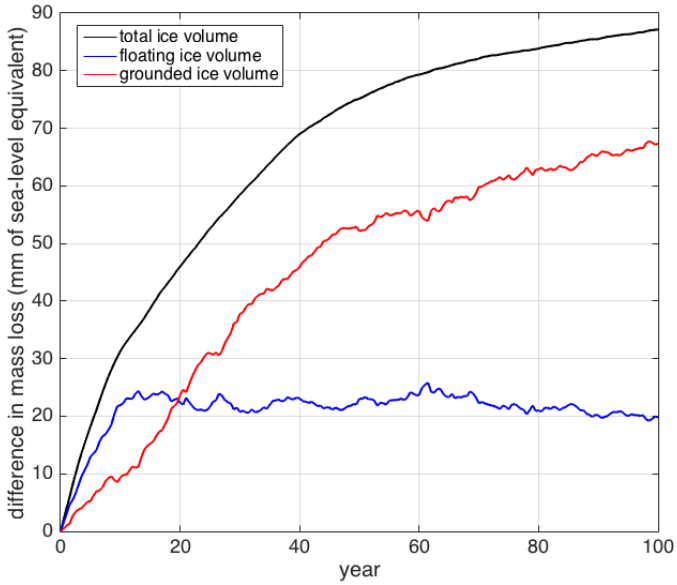

Figure 7. Difference in total ice volume loss (in units of equivalent mm of sea-level change) when Antarctic ice sheet model is forced using submarine melt rates diagnosed from the simulation with perturbed Southern Ocean winds versus the control simulation (positive units indicate greater mass loss for the perturbed winds simulation).

4.0 References

Fürst, JJ, G Durand, F Gillet-Chaulet, L Tavard, M Rankl, M Braun, and O Gagliardini, 2016: The safety band of Antarctic ice shelves. *Nature Climate Change*, **6**, 479–482, doi:10.1038/nclimate2912.

Fyfe, JC, OA Saenko, K Zickfeld, M Eby, and AJ Weaver, 2007: The Role of Poleward-Intensifying Winds on Southern Ocean Warming. *J Climate*, **20**, 5391–5400, doi:10.1175/2007JCLI1764.1.

Griffies, SM, et al., 2009: Coordinated Ocean-ice Reference Experiments (COREs), *Ocean Modell.*, **26**, 1–46.

Gudmundsson, GH, 2013: Ice-shelf buttressing and the stability of marine ice sheets. *The Cryosphere*, **7**, 647–655, doi:10.5194/tc-7-647-2013.

Hellmer, HH, F Kauker, R Timmermann, J Determann, and J Rae, 2012: Twenty-first-century warming of a large Antarctic ice-shelf cavity by a redirected coastal current. *Nature*, **485**, 225–228, doi:10.1038/nature11064.

Holland, D, and A Jenkins, 1999: Modeling thermodynamic ice–ocean interactions at the base of an ice shelf. *Journal of Physical Oceanography*, **29**, 1787–1800.

Jacobs, SS, A Jenkins, CF Giulivi, and P Dutrieux, 2011: Stronger ocean circulation and increased melting under Pine Island Glacier ice shelf. *Nature Geoscience*, **4**, 519–523, doi:10.1038/ngeo1188.

Jenkins, A, KW Nicholls, and HFJ Corr, 2010: Observation and Parameterization of Ablation at the Base of Ronne Ice Shelf, Antarctica. *Journal of Physical Oceanography*, **40**, 2298–2312, doi:10.1175/2010JPO4317.1.

Scambos, T, J Bohlander, C Shuman, and P Skvarca, 2004: Glacier acceleration and thinning after ice shelf collapse in the Larsen B embayment, Antarctica. *Geophys. Res. Lett*, **31**, 18.

Spence, P, SM Griffies, and MH England, 2014: Rapid subsurface warming and circulation changes of Antarctic coastal waters by poleward shifting winds. *Geophys. Res. Lett.*, **41**, 4601-4610, doi:10.1002/(ISSN)1944-8007.

Thompson, DWJ, and S Solomon, 2002: Interpretation of Recent Southern Hemisphere Climate Change. *Science*, **296**, 895–899.

Large, WG, and SG Yeager, 2008: The global climatology of an interannually varying air–sea flux data set. *Clim Dyn*, **33**, 341–364, doi:10.1007/s00382-008-0441-3.

Zheng, F, J Li, RT Clark, and HC Nnamchi, 2013: Simulation and Projection of the Southern Hemisphere Annular Mode in CMIP5 Models. *J Climate*, **26**, 9860–9879, doi:10.1175/JCLI-D-13-00204.1.

U.S. DEPARTMENT OF
ENERGY

Office of Science